ANALYSIS OF THE WHEEL ORIENTATION ANGLES IN LOCKHEED F-104S STARFIGHTER AIRCRAFT

Damian Brewczyński, Grzegorz Tora

CracowUniversity of Technology
Faculty of Mechanical Engineering
Institute of Machine Design
Jana Pawła II Av. 37, 31-864 Krakow, Poland
tel.: +48 12 6283408, fax: +48 12 3743360
e-mail:brewczyn@mech.pk.edu.pl, tora@mech.pk.edu.pl

Abstract

This article contains kinematic analysis of the chassis mechanism used in Lockheed F-104S Star fighter aircraft, which is recently used by the NATO military aviation as an interceptor. The mechanism of the chassis is made up of several smaller subsystems with different functions. The first mechanism is used to eject the chassis before landing (touchdown) and fold it to hatchway after the lift off. The second mechanism is designed to perform rotation of the crossover with the wheel, in order to adjust the position of the wheel to fit it in the limited space in the hold. The third mechanism allows movement of the chassis resulting from the change in length of the damper. To determine the position of the following links of the mechanism was used calculus of vectors in which unit vectors were used to represent the angular position of the links. Often used equation, which describes a polygon vector, and the equation of unknown unit vector possible to determine if the other two and the angles between them are known. Calculations were performed in the three local systems of reference, thus were obtained the simplest forms of solutions for links positions. The corresponding scalar products of unit vectors are elements of two transition matrices. These matrices are needed for the vectors calculation in each of the three coordinate systems. The result of the analysis is to determine the angle of convergence and the angle of heel wheels as a function of variable length of hydraulic cylinder and the length of the shock absorber. It has been shown that length of the shock absorber has little effect on angle of convergence, but has a significant effect on the angle of the tilt-wheel landing gear.

Keywords: *mechanical engineering, aircraft engineering, kinematic analysis*

1. Introduction

A typical solution in the construction of the current aircraft flight decreasing resistance is the mechanism comprising movable chassis to hatch located in the body of the aircraft. In used until recently by the NATO military aviation as a fighter interceptor, movable main landing gear is located in the central part of the fuselage.

The paper contains a kinematic analysis of the spatial mechanism chassis in a range of positions. The analysis determined convergence angle and the angle of heel landing wheels as a function of chassis extendible hydraulic cylinder length and the length of the shock absorber.
The analysis was performed using a vector method using versors representing the angular position of the links [1, 4].

2. Construction of the landing gear mechanism

Gear mechanism consists of a three smaller mechanisms that perform different functions [2]. The first mechanism is used to eject the landing gear before landing and folding it after lift-off (Fig. 1). It consists of two fixed-length links 2 and 3 and the hydraulic cylinder 4, connected to a double pivot *D*. The shank is connected by pivot *E* to the actuator and by pivot *C* to link 2. To connect link 3 to the airframe were used movable link 10. Link 10 is connected with link 3 by

pivot *B* and with airplane frame by pivot *N*. Rotary joint axes *A, B, C, D* and *E* are parallel to each other, so that part of the chassis, composed of links 3, 2, shank 1 and the actuator 4 can be regarded as a flat mechanism.

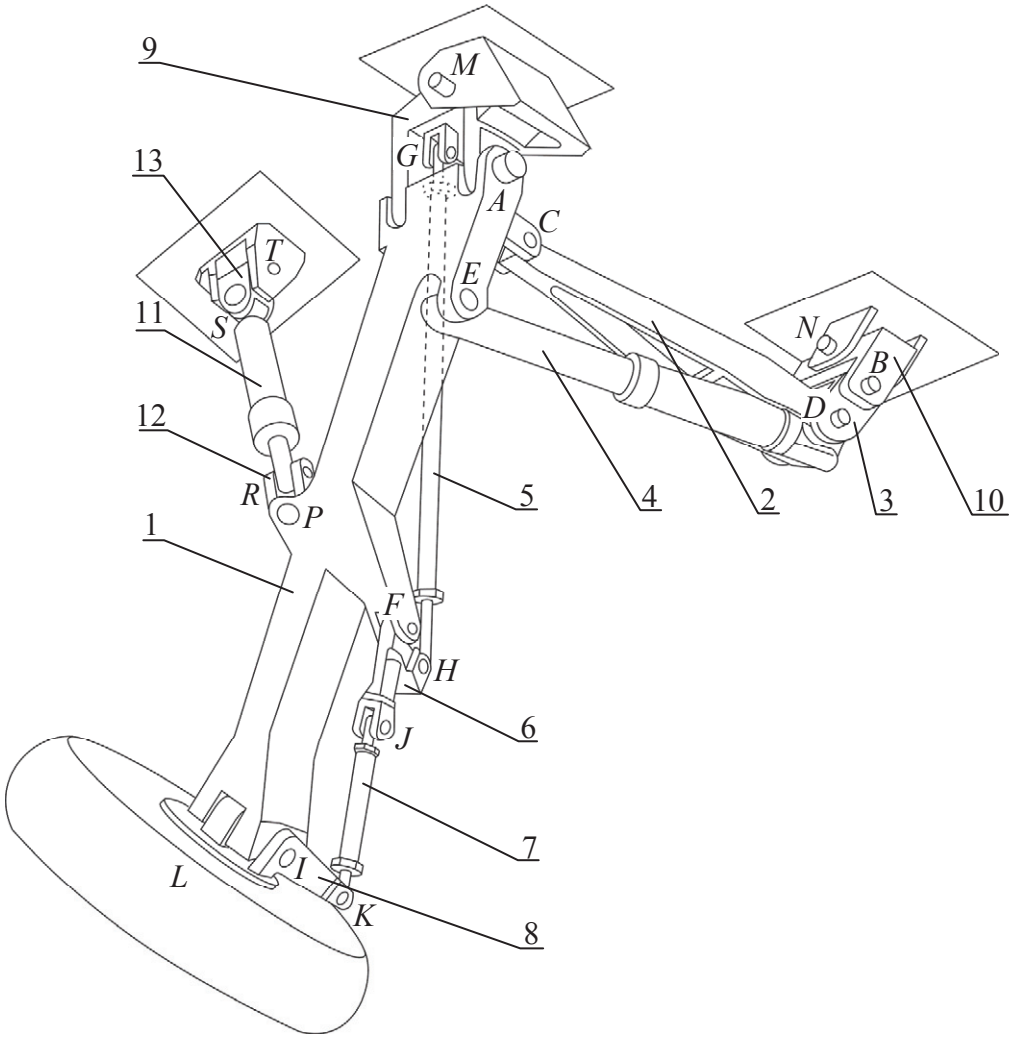

Fig. 1. The mechanism of the Lockheed F-104S Starfighter landing gear

The second gear mechanism is designed to perform a limited rotation of the steering 8 with the wheel around pivot *I* caused by movement of the shank 1. The rotation around the axis of pivot *I* should provide accurate positioning of the wheel in two extreme positions. The first results from the necessity of such a setting is wheel to be able to fold and fit in to the expected area of the chassis hatch. The second extreme position refers to the total distribution of the chassis, where the wheel should achieve established angle to the shank. Rotate the wheel steering joint *I* is forced by the space arrangement of two quadrangle, connected to the shank.

The first quadrangle is made up of connector 9, shank 1, connector 5 and wishbone 6. Wishbone 6 is connected to the shank by pivot *F*. Link 5 is connected to the connector 9 and the wishbone 6 by ball joints *G* and *H*. The second quadrangle consists of wishbone 6, shank 1, connector 7 and steering 8. The steering 8 is connected to the shank by joint *I*. Link 7 is connected to the wishbone 6 and steering 8 by ball joints *J* and *K*. The main landing gear wheel is mounted on the pivot 8 in the rotary joint *L*. Changing the length of the actuator 4 movable landing gear mechanism rotates the main shank 1 around the pivot *al* and simultaneous rotation of steering 8 wheel around pivot axis *I*. In mechanism of movable chassis connectors 5 and 7 has adjustable length. The use of such regulation compensates for inaccuracies performance of links and their assembly to ensure accurate positioning of the wheels in the extreme positions.

The third mechanism allows movement of the chassis resulting from a change in the length of the elastic damping (hereinafter referred to as shock absorber) 11. Shank is connected indirectly to the airframe by a movable connector 9, connected to the plane frame by pivot *M* and to the shank by pivot *A*. Shock absorber 11 is positioned over the shank connected thereto and to the plane frame by means of connectors 12 and 13. Connector 12 is connected to the shank 1 by pivot *P*, and to shock absorber by pivot *R*. Connector 13 is connected to the frame pivot plane *T*, and shock absorber pivot *S*. During take-off and landing aircraft, as a result of changes in the length of shank damper rotates around a pivot axis *M*. Joints *M* and *N* have a common axis of rotation which is parallel to the line of intersection of the plane symmetry and the surface on which the aircraft is.

The landing gear mechanism cooperating with the opening and closing mechanisms of the two flaps. These mechanisms are not shown in Figure 1 and are not considered in this study.

3. Analysis of links positions in the landing gear mechanism

Each of the three mechanisms is described in their own reference systems in which they determined the position of the links. The first reference system $\{A_g x_g y_g z_g\}$ is related to the shank 1 (Fig. 2). Axis z_g lies in the pivot axis *A*. Axis x_g intersects at straight angle joint axes *A* and *E*. The centre A_g is the point of intersection of pivot axis *A* and perpendicular to the surface containing the centre of the ball joint *G*.

A second reference system – $\{A_s s_i s_t s\}$ is related to switches 9 and 10, which perform a rotation about a common pivot axis *M* and *N* (Fig. 2 and 3). Axis *with* the axis z_g and x_g axis inter sects a perpendicular pivot axes *A* and *E*. Points A_s and A_g overlap. In this reference system, displacements of the wheel orienting mechanism links are calculate.

The third reference system $\{O_m x_m y_m z_m\}$ is related with the plane frame (Fig. 3 and 4). Axis x_m lies on a common pivot axis *M* and d*N*. Axis z_m is perpendicular to the surface on which the aircraft stands. O_m point lies at the intersection of axis x_m with the surface $z_m y_m$ containing the point of intersection of the pivot *T* of a straight line intersecting at a right angle joint axes *T* and *S*. In this reference system calculates the shank displacement including wheel resulting from the change in length of the shock absorber the taper angle δ and the tilt angle of the wheel ε. Wanted wheel orientation angles are determined in the system $\{O_m x_m y_m z_m\}$. In a previous analysis, versors are determined reference system $\{A_g x_g y_g z_g\}$ and $\{A_s s_i s_t s\}$.It is therefore necessary to find transition matrix between two pairs of subsequent reference systems. Symbols versors expressed in systems $\{A_g x_g y_g z_g\}$, $\{A_s s_i s_t s\}$ and $\{O_m x_m y_m z_m\}$ contain the upper left index of "*g*", "*s*" or "*m*".

3.1. Links positions analysis of the chassis eject mechanism

Position analysis of the landing gear ejecting mechanism has the task to determine in the system $\{A_g x_g y_g z_g\}$versors of moving links, especially versor ${}^g\boldsymbol{i}_{sx}^0$lying straight line passing through the joint axes *A* and *B* which is the axis x_s of the reference system $\{A_s s_i s_t s\}$.

In the flat ejecting chassis mechanism versors describing the angular position of links are parallel to the surface $x_s y_s$. Based on the triangle *CDE* (Fig. 2) formulate a relationship:

$$l_2\ {}^g\boldsymbol{i}_2^0 + S_4\ {}^g\boldsymbol{i}_4^0 = l_{CE}\ {}^g\boldsymbol{i}_{1CE}^0, \tag{1}$$

which is the basis for determining versors:

$${}^g\boldsymbol{i}_2^0 = \sqrt{1 - \left(\frac{l_2^2 - S_4^2 + l_{CE}^2}{2 l_{CE} l_2}\right)^2}\ {}^g\boldsymbol{f}_1^0 + \frac{l_2^2 - S_4^2 + l_{CE}^2}{2 l_{CE} l_2}\ {}^g\boldsymbol{i}_{1CE}^0, \tag{2}$$

where:

${}^g\boldsymbol{i}_{1CE}^0$– –versor associated with the shank with known coordinates,
${}^g\boldsymbol{f}_1^0$ – versor perpendicular to the ${}^g\boldsymbol{i}_{1CE}^0$, l_2, l_{CE} – constant links size,
S_4 – temporary length of the actuator 4.

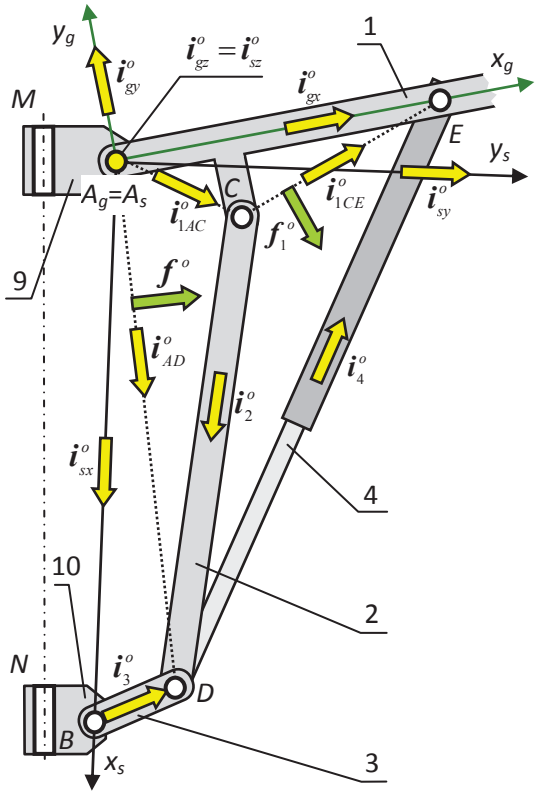

Fig. 2. Chassis eject mechanism

Triangle *ACD* can be described by the equation:

$$l_{AC}\ {}^{g}\boldsymbol{i}^0_{1AC} + l_2\ {}^{g}\boldsymbol{i}^0_2 = S_{AD}\ {}^{g}\boldsymbol{i}^0_{AD}, \tag{3}$$

which set a distance between the axes of the joints *A* and *D* and the versor in the direction of *AD*:

$$S_{AD} = \sqrt{l^2_{AC} + l^2_2 + 2l_2\ l_{AC}\left({}^{g}\boldsymbol{i}^0_{1AC} \cdot {}^{g}\boldsymbol{i}^0_2\right)},\ {}^{g}\boldsymbol{i}^0_{AD} = \frac{l_{1AC}\ {}^{g}\boldsymbol{i}^0_{1AC} + l_2\ {}^{g}\boldsymbol{i}^0_2}{S_{AD}}, \tag{4}$$

where:

${}^{g}\boldsymbol{i}^0_{1AC}$ – versor associated with the shank with known coordinates,

l_{AC} – shank dimension.

Based on the triangle *ABD* can write:

$$l_{AB}\ {}^{g}\boldsymbol{i}^0_{sx} + l_3\ {}^{g}\boldsymbol{i}^0_3 = S_{AD}\ {}^{g}\boldsymbol{i}^0_{AD}, \tag{5}$$

where it is determined versors:

$${}^{g}\boldsymbol{i}^0_{sx} = \sqrt{1 - \left(\frac{l^2_{AB} - l^2_3 + S^2_{AD}}{2S_{AD}l_{AB}}\right)^2}\ {}^{g}\boldsymbol{f}^0 + \frac{l^2_{AB} - l^2_3 + S^2_{AD}}{2S_{AD}l_{AB}}\ {}^{g}\boldsymbol{i}^0_{AD}, \tag{6}$$

where: ${}^{g}\boldsymbol{f}^0$ – versor perpendicular to the ${}^{g}\boldsymbol{i}^0_{AD}$, l_3, l_{AB} – constant links size.

Determination of the ${}^{g}\boldsymbol{i}^0_{sx}$ determines the transition matrix from the reference system $\{A_g x_g y_g z_g\}$ to the $\{A_s s_i s_t s\}$:

$${}^{s}_{g}\boldsymbol{R} = \begin{bmatrix} {}^{g}\boldsymbol{i}^0_{gx} \cdot {}^{g}\boldsymbol{i}^0_{sx} & {}^{g}\boldsymbol{i}^0_{gy} \cdot {}^{g}\boldsymbol{i}^0_{sx} & 0 \\ {}^{g}\boldsymbol{i}^0_{gx} \cdot {}^{g}\boldsymbol{i}^0_{sy} & {}^{g}\boldsymbol{i}^0_{gy} \cdot {}^{g}\boldsymbol{i}^0_{sy} & 0 \\ 0 & 0 & 1 \end{bmatrix}, \tag{7}$$

where: ${}^{g}\boldsymbol{i}^0_{gx} = [1,0,0]^T$, ${}^{g}\boldsymbol{i}^0_{gy} = [0,1,0]^T$, ${}^{g}\boldsymbol{i}^0_{sz} = [0,0,1]^T$, ${}^{g}\boldsymbol{i}^0_{sy} = {}^{g}\boldsymbol{i}^0_{sz} \times {}^{g}\boldsymbol{i}^0_{sx}$.

3.2. Links positions analysis of the wheel turning mechanism

The rotating wheel mechanism which motion is forced by the rotation of the main shank around the pivot axis A is a combination of two spatial quadrangle *RSSR* type [3].

Links positions analysis result of the rotating wheel mechanism is determined directional versor ${}^{s}\boldsymbol{i}_{n}^{0}$ of the wheel plane expressed in system $\{A_s x_s y_s z_s\}$.

Point F_1 is located at the intersection of the pivot axis F, and the perpendicular plane containing the ball joint centre H [5]. Point I_1, is located at the intersection of the pivot axis I and a perpendicular plane containing ball joint centre K.

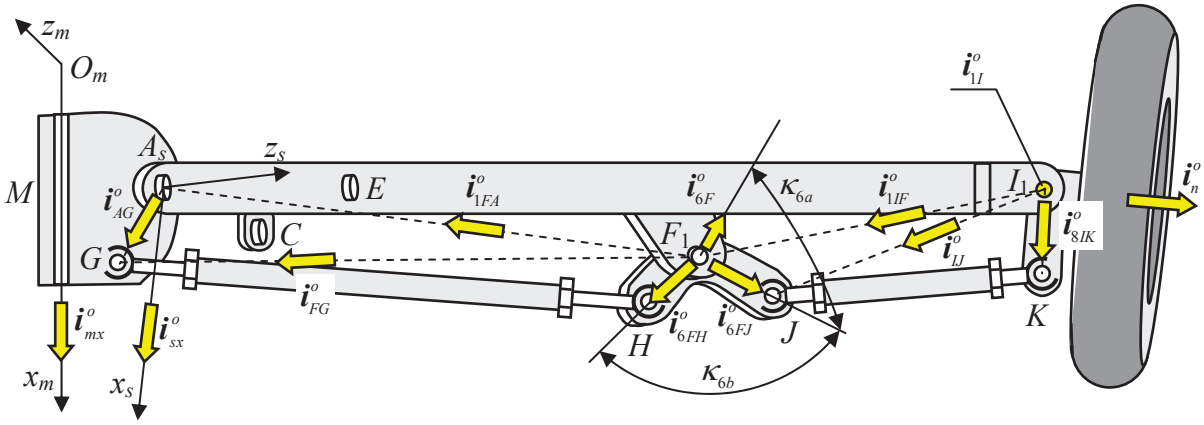

Fig. 3. The chassis mechanism that causes rotation of the steering wheel

Triangle $F_1 A_s G$ can be described by the equation:

$$l_{FA}\ {}^{s}\boldsymbol{i}_{1FA}^{0} + l_{AG}\ {}^{s}\boldsymbol{i}_{AG}^{0} = S_{FG}\ {}^{s}\boldsymbol{i}_{FG}^{0}, \tag{8}$$

where: ${}^{s}\boldsymbol{i}_{1FA}^{0} = {}_{g}^{s}\boldsymbol{R}\ {}^{g}\boldsymbol{i}_{1FA}^{0}$,

which set a variable distance between F_1 and G and the versor in the direction of F_1G:

$$S_{FG} = \sqrt{l_{AG}^2 + l_{FA}^2 + 2 l_{AG} l_{FA}\left({}^{s}\boldsymbol{i}_{1AG}^{0} \cdot {}^{s}\boldsymbol{i}_{1FA}^{0}\right)},\ {}^{s}\boldsymbol{i}_{FG}^{0} = \frac{l_{AG}\ {}^{s}\boldsymbol{i}_{AG}^{0} + l_{FA}\ {}^{s}\boldsymbol{i}_{1FA}^{0}}{S_{FG}}, \tag{9}$$

where: ${}^{s}\boldsymbol{i}_{AG}^{0}$ – known versor in the direction of A_sG, l_{AG}, l_{FA} known dimensions of the links.

The resulting values are base to designate versor associated with the wishbone 6:

$${}^{s}\boldsymbol{i}_{6FH}^{0} = \frac{c_{2a} - c_{1a}c_{3a}}{1 - c_{1a}^2}\ {}^{s}\boldsymbol{i}_{6F}^{0} + \frac{c_{3a} - c_{1a}c_{2a}}{1 - c_{1a}^2}\ {}^{s}\boldsymbol{i}_{FG}^{0} \pm \frac{\sqrt{1 - c_{1a}^2 - c_{2a}^2 - c_{3a}^2 + 2c_{1a}c_{2a}c_{3a}}}{1 - c_{1a}^2}\left({}^{s}\boldsymbol{i}_{6F}^{0} \times {}^{s}\boldsymbol{i}_{FG}^{0}\right), \tag{10}$$

where: ${}^{s}\boldsymbol{i}_{6F}^{0} = {}_{g}^{s}\boldsymbol{R}\ {}^{g}\boldsymbol{i}_{6F}^{0}$, ${}^{g}\boldsymbol{i}_{6F}^{0}$ – a known direction of the pivot F axis versor, $c_{1a} = {}^{s}\boldsymbol{i}_{6F}^{0} \cdot {}^{s}\boldsymbol{i}_{FG}^{0}$,

$c_{2a} = {}^{s}\boldsymbol{i}_{6F}^{0} \cdot {}^{s}\boldsymbol{i}_{6FH}^{0} = cos\frac{\pi}{2} = 0$, $c_{3a} = {}^{s}\boldsymbol{i}_{6FH}^{0} \cdot {}^{s}\boldsymbol{i}_{FG}^{0} = \frac{S_{FG}^2 + l_{FH}^2 - l_5^2}{2 S_{FG} l_{FH}}$.

Another versor associated with the wishbone 6 is:

$${}^{s}\boldsymbol{i}_{6FJ}^{0} = \frac{c_{2b} - c_{1b}c_{3b}}{1 - c_{1b}^2}\ {}^{s}\boldsymbol{i}_{6F}^{0} + \frac{c_{3b} - c_{1b}c_{2b}}{1 - c_{1b}^2}\ {}^{s}\boldsymbol{i}_{6FH}^{0} \pm \frac{\sqrt{1 - c_{1b}^2 - c_{2b}^2 - c_{3b}^2 + 2c_{1b}c_{2b}c_{3b}}}{1 - c_{1b}^2}\left({}^{s}\boldsymbol{i}_{6F}^{0} \times {}^{s}\boldsymbol{i}_{FH}^{0}\right), \tag{11}$$

where:

$c_{1b} = {}^{s}\boldsymbol{i}_{6F}^{0} \cdot {}^{s}\boldsymbol{i}_{6FH}^{0} = cos\frac{\pi}{2} = 0$, $c_{2b} = {}^{s}\boldsymbol{i}_{6F}^{0} \cdot {}^{s}\boldsymbol{i}_{6FJ}^{0} = cos\kappa_{6a}$,

$c_{3b} = {}^{s}\boldsymbol{i}_{6FH}^{0} \cdot {}^{s}\boldsymbol{i}_{6FJ}^{0} = cos\kappa_{6b}$, κ_{6a}– fixed angle between the segment F_1J and the pivot F,

κ_{6b} – fixed angle between segments F_1J and F_1H.

Triangle I1F1J can be described by the relationship:

$$l_{IF}\ {}^{s}\boldsymbol{i}_{IF}^{0} + l_{FJ}\ {}^{s}\boldsymbol{i}_{6FJ}^{0} = S_{IJ}\ {}^{s}\boldsymbol{i}_{IJ}^{0}, \tag{12}$$

which set a variable distance between I_1 and J and the versor on direction I_1J:

$$S_{IJ} = \sqrt{l_{IF}^2 + l_{FJ}^2 + 2l_{IF}l_{FJ}\left({}^{s}\boldsymbol{i}_{1IF}^{0} \cdot {}^{s}\boldsymbol{i}_{6FJ}^{0}\right)},\ {}^{s}\boldsymbol{i}_{IJ}^{0} = \frac{l_{IF}\ {}^{s}\boldsymbol{i}_{1IF}^{0} + l_{FJ}\ {}^{s}\boldsymbol{i}_{6FJ}^{0}}{S_{IJ}}, \tag{13}$$

where: ${}^{s}\boldsymbol{i}_{1IF}^{0} = {}_{g}^{s}\boldsymbol{R}\ {}^{g}\boldsymbol{i}_{1IF}^{0}$, ${}^{g}\boldsymbol{i}_{1IF}^{0}$ – known versor on direction I_1F_1, l_{IF} ,l_{FJ}, – dimensions of the links.

Versor on the pivot 8 can be expressed as:

$${}^{s}\boldsymbol{i}_{8IK}^{0} = \frac{c_{2c}-c_{1c}c_{3c}}{1-c_{1c}^2}\ {}^{s}\boldsymbol{i}_{IJ}^{0} + \frac{c_{3c}-c_{1c}c_{2c}}{1-c_{1c}^2}\ {}^{s}\boldsymbol{i}_{1I}^{0} \pm \frac{\sqrt{1-c_{1c}^2-c_{2c}^2-c_{3c}^2+2c_{1c}c_{2c}c_{3c}}}{1-c_{1c}^2}\left({}^{s}\boldsymbol{i}_{IJ}^{0} \times {}^{s}\boldsymbol{i}_{1I}^{0}\right), \tag{14}$$

where: ${}^{s}\boldsymbol{i}_{1I}^{0} = {}_{g}^{s}\boldsymbol{R}\ {}^{g}\boldsymbol{i}_{1I}^{0}$, ${}^{g}\boldsymbol{i}_{1I}^{0}$ – known versor pivot axis I, $c_{1c} = {}^{s}\boldsymbol{i}_{IJ}^{0} \cdot {}^{s}\boldsymbol{i}_{1I}^{0}$, $c_{2c} = {}^{s}\boldsymbol{i}_{IJ}^{0} \cdot {}^{s}\boldsymbol{i}_{8IK}^{0} = \frac{S_{IJ}^2+l_{8IK}^2-l_7^2}{2S_{IJ}l_{8IK}}$, $c_{3c} = {}^{s}\boldsymbol{i}_{1I}^{0} \cdot {}^{s}\boldsymbol{i}_{8IK}^{0} = cos\frac{\pi}{2} = 0$.

Perpendicular to each other versors $\boldsymbol{i}_{1I}^{0}$and $\boldsymbol{i}_{8IK}^{0}$are both parallel to the plane of the wheel. Directional Versor in the wheel plane in system $\{A_sx_sy_sz_s\}$ is:

$${}^{s}\boldsymbol{i}_{n}^{0} = {}^{s}\boldsymbol{i}_{1I}^{0} \times {}^{s}\boldsymbol{i}_{8IK}^{0}. \tag{15}$$

3.3. Analysis of wheel angular position consequent from the change in length of the shock absorber

The chassis links movement with locked cylinder 4 at its maximum length, due to dynamic loads that occur during take-off and landing. Reduced load applied to the shock absorber 11 affects its temporary length and the angular position on shank 1 and wheel orientation. In order to determine the orientation angles of the wheels should designate transition matrix from reference system $\{A_sx_sy_sz_s\}$ associated with the links 9 and 10 and system connected to the plane frame $\{O_mx_my_mz_m\}$.Transition matrix elements dependent on η -the distance between points T_{13} and P_{12}. Points T_{13} and S_{13} lies on the axis of rotation joints T and S of connector 13 and the straight line intersecting these axes at right angles. P_{12} and R_{12} points lies on the axes of rotation joints P and $R$of link 12 and the straight line intersecting these axes at right angles.

At the time of changing the length of shock absorber lending gear rotates about a common axis of pivot joints M and N, which determines versor ${}^{s}\boldsymbol{i}_{mx}^{0}$known in $\{A_sx_sy_sz_s\}$ system which is parallel to the surface of symmetry of the plane and the surface on which the aircraft is.

Versor on direction O_mP_{12}:

$${}^{m}\boldsymbol{i}_{OP}^{0} = \frac{c_{2d}-c_{1d}c_{3d}}{1-c_{1d}^2}\ {}^{m}\boldsymbol{i}_{T}^{0} + \frac{c_{3d}-c_{1d}c_{2d}}{1-c_{1d}^2}\ {}^{m}\boldsymbol{i}_{mx}^{0} \pm \frac{\sqrt{1-c_{1d}^2-c_{2d}^2-c_{3d}^2+2c_{1d}c_{2d}c_{3d}}}{1-c_{1d}^2}\left({}^{m}\boldsymbol{i}_{T}^{0} \times {}^{m}\boldsymbol{i}_{mx}^{0}\right), \tag{16}$$

where:

${}^{m}\boldsymbol{i}_{T}^{0} = \left[0, {}^{m}\boldsymbol{i}_{Ty}^{0}, {}^{m}\boldsymbol{i}_{Tz}^{0}\right]^T$ – known versor on direction O_mT_{13}, ${}^{m}\boldsymbol{i}_{mx}^{0} = [1,0,0]^T$, $c_{1d} = cos < \left(\boldsymbol{i}_{T}^{0}, \boldsymbol{i}_{mx}^{0}\right) = 0$

$c_{2d} = \frac{l_{O_mT}^2+l_{O_mP}^2-\eta^2}{2l_{O_mT}l_{O_mP}}$, $c_{3d} = cos\ \kappa_{1d}$, κ_{1d} – fixed angle between versors ${}^{m}\boldsymbol{i}_{OP}^{0}$ and ${}^{m}\boldsymbol{i}_{mx}^{0}$.

Versor on direction O_mA:

$${}^{m}\boldsymbol{i}_{OA}^{0} = \frac{c_{2e}-c_{1e}c_{3e}}{1-c_{1e}^2}\ {}^{m}\boldsymbol{i}_{mx}^{0} + \frac{c_{3e}-c_{1e}c_{2e}}{1-c_{1e}^2}\ {}^{m}\boldsymbol{i}_{OP}^{0} \pm \frac{\sqrt{1-c_{1e}^2-c_{2e}^2-c_{3e}^2+2c_{1e}c_{2e}c_{3e}}}{1-c_{1e}^2}\left({}^{m}\boldsymbol{i}_{mx}^{0} \times {}^{m}\boldsymbol{i}_{OP}^{0}\right) \tag{17}$$

where: $c_{1e} = {}^{m}\boldsymbol{i}_{mx}^{0} \cdot {}^{m}\boldsymbol{i}_{OP}^{0}$,$c_{2e} = \frac{l_{O_mM}^2+l_{O_mA}^2-l_{AM}^2}{2l_{O_mM}l_{O_mA}}$,$c_{3e} = \frac{l_{O_mA}^2+l_{O_mP_{12}}^2-l_{AP_{12}}^2}{2l_{O_mA}l_{O_mP_{12}}}$.

Versor on direction AP_{12}:

$$ {}^{m}\boldsymbol{i}_{AP}^{0} = \frac{{}^{m}i_{OP}^{0} l_{O_m P_{12}} - {}^{m}i_{OA}^{0} l_{O_m A}}{l_{AP_{12}}}. \tag{18} $$

Axis z_s versor:

$$ {}^{m}\boldsymbol{i}_{sz}^{0} = \frac{c_{2f} - c_{1f}c_{3f}}{1-c_{1f}^{2}} {}^{m}\boldsymbol{i}_{mx}^{0} + \frac{c_{3f} - c_{1f}c_{2f}}{1-c_{1f}^{2}} {}^{m}\boldsymbol{i}_{AP}^{0} \pm \frac{\sqrt{1-c_{1f}^{2}-c_{2f}^{2}-c_{3f}^{2}+2c_{1f}c_{2f}c_{3f}}}{1-c_{1f}^{2}} ({}^{m}\boldsymbol{i}_{mx}^{0} \times {}^{m}\boldsymbol{i}_{AP}^{0}). \tag{19} $$

where: $c_{1f} = cos\ \ \kappa_{1f}$, κ_{1f} – fixed angle between versors ${}^{m}\boldsymbol{i}_{AP}^{0}$ and ${}^{m}\boldsymbol{i}_{mx}^{0}$,
$c_{2f} = cos < (\ \boldsymbol{i}_{sz}^{0},\ \boldsymbol{i}_{mx}^{0}) = 0, c_{3f} = cos\ \ \kappa_{2f}$, κ_{2f} – fixed angle between versors $\boldsymbol{i}_{sz}^{0}$ i $\boldsymbol{i}_{AP}^{0}$.

Axis x_s versor:

$$ {}^{m}\boldsymbol{i}_{sx}^{0} = \frac{c_{2g} - c_{1g}c_{3g}}{1-c_{1g}^{2}} {}^{m}\boldsymbol{i}_{sz}^{0} + \frac{c_{3g} - c_{1g}c_{2g}}{1-c_{1g}^{2}} {}^{m}\boldsymbol{i}_{AP}^{0} \pm \frac{\sqrt{1-c_{1g}^{2}-c_{2g}^{2}-c_{3g}^{2}+2c_{1g}c_{2g}c_{3g}}}{1-c_{1g}^{2}} ({}^{m}\boldsymbol{i}_{sz}^{0} \times {}^{m}\boldsymbol{i}_{AP}^{0}), \tag{20} $$

where: $c_{1g} = cos\ \ \kappa_{2f}$, $c_{2g} = cos < (\ \boldsymbol{i}_{sz}^{0},\ \boldsymbol{i}_{sx}^{0}) = 0, c_{1g} = cos\ \ \kappa_{1g}$, κ_{1g} – fixed angle between versors $\boldsymbol{i}_{sx}^{0}$ i $\boldsymbol{i}_{AP}^{0}$.

Transition matrix from reference system $\{A_s x_s y_s z_s\}$ to the system $\{O_m x_m y_m z_m\}$:

$$ {}^{m}_{s}\boldsymbol{R} = \begin{bmatrix} {}^{m}\boldsymbol{i}_{sx}^{0} \cdot {}^{m}\boldsymbol{i}_{mx}^{0} & {}^{m}\boldsymbol{i}_{sy}^{0} \cdot {}^{m}\boldsymbol{i}_{mx}^{0} & {}^{m}\boldsymbol{i}_{sz}^{0} \cdot {}^{m}\boldsymbol{i}_{mx}^{0} \\ {}^{m}\boldsymbol{i}_{sx}^{0} \cdot {}^{m}\boldsymbol{i}_{my}^{0} & {}^{m}\boldsymbol{i}_{sy}^{0} \cdot {}^{m}\boldsymbol{i}_{my}^{0} & {}^{m}\boldsymbol{i}_{sz}^{0} \cdot {}^{m}\boldsymbol{i}_{my}^{0} \\ {}^{m}\boldsymbol{i}_{sx}^{0} \cdot {}^{m}\boldsymbol{i}_{mz}^{0} & {}^{m}\boldsymbol{i}_{sy}^{0} \cdot {}^{m}\boldsymbol{i}_{mz}^{0} & {}^{m}\boldsymbol{i}_{sz}^{0} \cdot {}^{m}\boldsymbol{i}_{mz}^{0} \end{bmatrix}, \tag{21} $$

where: ${}^{m}\boldsymbol{i}_{mx}^{0} = [1,0,0]^{T}$, ${}^{m}\boldsymbol{i}_{my}^{0} = [0,1,0]^{T}$, ${}^{m}\boldsymbol{i}_{mz}^{0} = [0,0,1]^{T}$, ${}^{m}\boldsymbol{i}_{sy}^{0} = {}^{m}\boldsymbol{i}_{sz}^{0} \times {}^{m}\boldsymbol{i}_{sx}^{0}$.

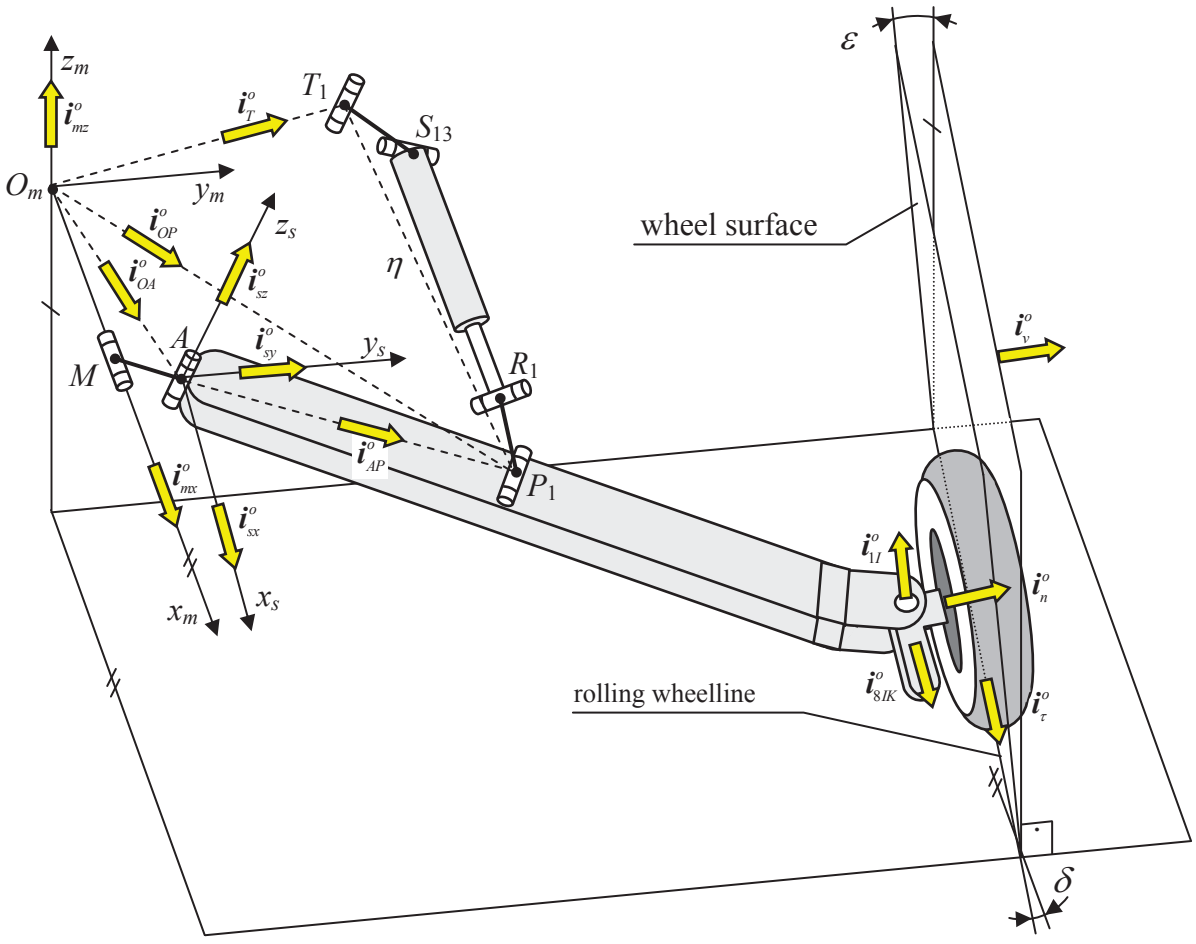

Fig. 4. The mechanism with shock absorber

4. Convergence and heel of wheel angles

Directional versor of wheel rolling line can be determined from the cross product of non-orthogonal versors $\boldsymbol{i}_n^0$ i $\boldsymbol{i}_{mz}^0$:

$$^m\boldsymbol{i}_\tau^0 = \frac{^m\boldsymbol{i}_n^0 \times {}^m\boldsymbol{i}_{mz}^0}{\left\| ^m\boldsymbol{i}_n^0 \times {}^m\boldsymbol{i}_{mz}^0 \right\|}, \tag{22}$$

where: $^m\boldsymbol{i}_n^0 = {}_s^m\boldsymbol{R}\ {}^s\boldsymbol{i}_n^0$.

Wheel convergence angle [6]:

$$\delta = sgn[^m\boldsymbol{i}_{mz}^0 \cdot (^m\boldsymbol{i}_\tau^0 \times {}^m\boldsymbol{i}_{mx}^0)]arcsin\left\| ^m\boldsymbol{i}_\tau^0 \times {}^m\boldsymbol{i}_{mx}^0 \right\|. \tag{23}$$

The angle of the tilt wheel [6]:

$$\varepsilon = sgn[^m\boldsymbol{i}_\tau^0 \cdot (^m\boldsymbol{i}_v^0 \times {}^m\boldsymbol{i}_n^0)]arcsin\left\| ^m\boldsymbol{i}_v^0 \times {}^m\boldsymbol{i}_n^0 \right\|, \tag{24}$$

where:

$^m\boldsymbol{i}_v^0 = {}^m\boldsymbol{i}_{mz}^0 \times {}^m\boldsymbol{i}_\tau^0$ – directional versor of plane perpendicular to the level containing the rolling line.

5. Results and conclusions

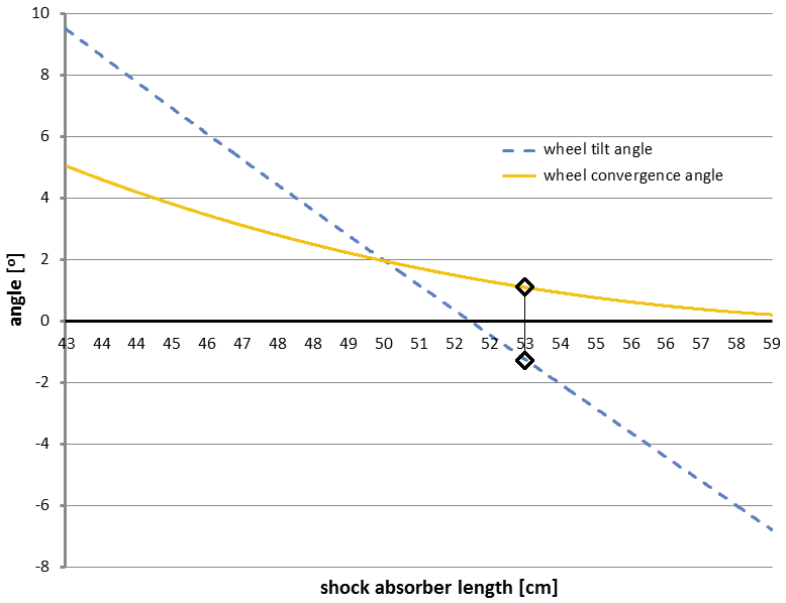

Fig5. Tilt angle and the angle of convergence of wheel as a function of the absorber length

Change the length of η in range (0.8-1.1) η_0 (where η_0 =0.53m – length for standing plane without an engine, fuel and armament) causes a change in the tilt angle ε in the range (9.2-6.0°) and change the taper angle δ in the range (4.9-0.3°).

Presented analysis can be the basis to examine the impact of accuracy of performance and links assembly mechanism on angular position of the wheel chassis. It can also be used to determine the extent of change in length of connectors 5 and 7 and performance compensation inaccuracy links assembly.

References

[1] Chace, M. A., *Solutions to the vector tetrahedron equation*, Transactions of the ASME, Journal of Engineering for Industry, Vol. 87, Series B, pp. 228-234, 1965.

[2] *Manuale tecnico catalog on o nomenclatore illustrato delle parti di ricambio VELIVOLO F-104S,* 1974.

[3] Cervantes-Sanchez, J. J., Moreno-Baez, M. A., Aguilera-Cortes, L. A., Gonzalez-Galvan, E. J., *Kinematic design of the RSSR-SC spatial linkage based on rotability conditions*, Mechanism and Machine Theory 40, pp. 1126-1144, 2005.
[4] Shigley, J. E., Uicker, J. J., *Theory of machines and mechanisms*, McGraw-Hill Book, 1995.
[5] Psang, Dain Lin, Jung-Fa, Hsieh, *A New Method to Analyze Spatial Binary Mechanisms with Spherical Pairs,* Journal of Mechanical Design, Vol. 129, pp. 455-458, 2007.
[6] Reimpell, J, Betzler, J., *Podwozia samochodów. Podstawy konstrukcji*, WKiŁ, Warszawa 2004.